Analysis of NDVI and scaled difference vegetation index retrievals of vegetation fraction

Article *in* Remote Sensing of Environment · April 2006

DOI: 10.1016/j.rse.2006.01.003

Available online at www.sciencedirect.com
SCIENCE DIRECT
Remote Sensing of Environment 101 (2006) 366–378
Remote Sensing of Environment
www.elsevier.com/locate/rse

Analysis of NDVI and scaled difference vegetation index retrievals of vegetation fraction

Zhangyan Jiang [a], Alfredo R. Huete [b], Jin Chen [a], Yunhao Chen [a,*], Jing Li [a], Guangjian Yan [c], Xiaoyu Zhang [c]

[a] Key Laboratory of Environmental Change and Natural Disaster Research of Education Ministry of China, College of Resources Science and Technology, Beijing Normal University, Beijing 100875, China
[b] Department of Soil, Water, and Environmental Science, University of Arizona, Tucson, AZ 85721, United States
[c] Center for Remote Sensing and GIS, Beijing Normal University, Beijing 100875, China

Received 24 May 2005; received in revised form 1 January 2006; accepted 8 January 2006

Abstract

The normalized difference vegetation index (NDVI) is the most widely used vegetation index for retrieval of vegetation canopy biophysical properties. Several studies have investigated the spatial scale dependencies of NDVI and the relationship between NDVI and fractional vegetation cover, but without any consensus on the two issues. The objectives of this paper are to analyze the spatial scale dependencies of NDVI and to analyze the relationship between NDVI and fractional vegetation cover at different resolutions based on linear spectral mixing models. Our results show strong spatial scale dependencies of NDVI over heterogeneous surfaces, indicating that NDVI values at different resolutions may not be comparable. The nonlinearity of NDVI over partially vegetated surfaces becomes prominent with darker soil backgrounds and with presence of shadow. Thus, the NDVI may not be suitable to infer vegetation fraction because of its nonlinearity and scale effects. We found that the scaled difference vegetation index (SDVI), a scale-invariant index based on linear spectral mixing of red and near-infrared reflectances, is a more suitable and robust approach for retrieval of vegetation fraction with remote sensing data, particularly over heterogeneous surfaces. The proposed method was validated with experimental field data, but further validation at the satellite level would be needed.

Keywords: NDVI; SDVI; Scale effect of NDVI; Vegetation fraction retrieval

1. Introduction

Vegetation is an important component of global ecosystems and knowledge of the Earth's vegetation cover is important to understand land-atmosphere interactions and their effects on climate. Changes in vegetation cover directly impact surface water and energy budgets through plant transpiration, surface albedo, emissivity, and roughness (Aman et al., 1992). Vegetation amount is usually parameterized through the fractional area of the vegetation occupying each grid cell (horizontal density) and the leaf area index (LAI), i.e., the number of leaf layers of the vegetated part (vertical density). Both evapotranspiration and photosynthesis are controlled by these two parameters (Gutman & Ignatov, 1998). Satellite data provide a spatially and periodic, comprehensive view of land vegetation cover. Several spectral vegetation indices have been developed over the last few decades which have been used to estimate vegetation canopy biophysical properties such as LAI, biomass and percent vegetation cover (Huete, 1988; Kaufman & Tanré, 1992; Liu & Huete, 1995; Richardson & Wiegand, 1977; Rouse et al., 1973; Tucker, 1979; Ünsalan & Boyer, 2004). Comparisons of the various vegetation indices can be found in Huete and Liu (1994), Elvidge and Chen (1995), Huete et al. (1997), McDonald et al. (1998) and Díaz and Blackburn (2003). Many remote sensing studies utilize vegetation indices to study vegetation, assuming that the properties of the background are constant or that soil variations are normalized by the particular vegetation index used (Hanan et al., 1991).

* Corresponding author. Tel.: +86 10 58806098; fax: +86 10 58807163.
E-mail addresses: Jzy@ires.cn (Z. Jiang), ahuete@ag.arizona.edu (A. Huete), Chenjin@ires.cn (J. Chen), cyh@ires.cn (Y. Chen),

0034-4257/$ - see front matter © 2006 Elsevier Inc. All rights reserved.
doi:10.1016/j.rse.2006.01.003

The normalized difference vegetation index (NDVI) is one of the most widely used vegetation indexes and its utility in satellite assessment and monitoring of global vegetation cover has been well demonstrated over the past two decades (Huete & Liu, 1994; Leprieur et al., 2000). It is defined as

$$\mathrm{NDVI} = \frac{N-R}{N+R} \quad (1)$$

where R and N represent surface reflectances averaged over visible ($\lambda \sim 0.6$ μm) and near infrared (NIR) ($\lambda \sim 0.8$ μm) regions of the spectrum, respectively. The NDVI is correlated with certain biophysical properties of the vegetation canopy, such as leaf area index (LAI), fractional vegetation cover, vegetation condition, and biomass. NDVI increases near-linearly with increasing LAI and then enters an asymptotic phase in which NDVI increases very slowly with increasing LAI. Several studies have found this asymptotic region pertains to a surface almost completely covered by leaves (Carlson & Ripley, 1997; Curran, 1983; Huete et al., 1985). Over densely vegetated surfaces, the NDVI responds primarily to red reflectances and is relatively insensitive to NIR variations, and hence unable to depict LAI variations (Huete et al., 1997). According to experimental measurements with different soil backgrounds (Huete et al., 1985), NDVI approach their maximum values at fractional vegetation covers between 80% and 90%. Similar experiments conducted by Díaz and Blackburn (2003) showed NDVI reaching asymptotic values at fractional vegetation covers of only 60%.

Carlson and Ripley (1997) distinguished between "local LAI", as measured in closed canopies and "global LAI" as would be measured without regard to the presence of breaks between the canopies. A local LAI would always equal or exceed the global LAI, and in partially vegetated, open canopies, the difference between global and local LAI may be considerable. It seems plausible that the variation of NDVI with respect to the global LAI in partially vegetated areas would be mostly controlled by the variation in the fraction of vegetated surface area illuminated by the sun and visible to the radiometer (Carlson & Ripley, 1997). Verstraete and Pinty (1991) discussed the nature and extent of NDVI variations in semi-arid lands, and argued that NDVI is more strongly controlled by changes in vegetation cover than by changes in the optical thickness of canopies. For partially vegetated landscapes, especially semi-arid areas, therefore, it is more direct and reasonable to derive vegetation fraction rather then LAI from NDVI.

Many researchers have investigated the relationship between NDVI and vegetation fraction and the retrieval of green vegetation fraction from NDVI. However, difficulties and uncertainties arise by the fact that one NDVI measurement does not allow simultaneous derivation of green vegetation fraction and local LAI. Gutman and Ignatov (1998) resolved this problem by prescribing local LAI equal to infinity and derived green vegetation cover from a scaled NDVI taken between bare soil NDVI and dense vegetation NDVI. Wittich and Hansing (1995) studied the relationship between NDVI and vegetation fraction at five test areas in Germany, and showed that, to a first approximation, the vegetation cover fraction was adequately described by the linear expression of NDVI over a wide distributed range of heterogeneous vegetation densities. Several other studies also showed a strong linear relation between fractional vegetation cover and NDVI (e.g. Kustas et al., 1993; Ormsby et al., 1987; Phulpin et al., 1990).

However, some investigations found the relationship between NDVI and vegetation fraction to be nonlinear with NDVI yielding distinct curves with vegetation cover changes corresponding to different soil types (e.g. Colwell, 1974; Huete et al., 1985). Using a linear mixture reflectance model, Hanan et al. (1991) found the NDVI of a mixed pixel to be dependent not only on the NDVI of pixel components and their proportions, but also on the brightness of the components. Dymond et al. (1992) found a nonlinear relationship between SPOT Haute Résolution Visible (HRV) derived NDVI and percent vegetation cover at a rangeland site in New Zealand. Choudhury et al. (1994) and Gillies and Carlson (1995) independently obtained identical square root relationships between the scaled NDVI and fractional vegetation cover. Carlson and Ripley (1997) used a simple radiative transfer model with vegetation, soil, and atmospheric components to illustrate the relation between NDVI, fractional vegetation cover, and LAI, and confirmed the square root relation. However, the reflectances of bare soil were fixed for all simulations in this model. So, the variations of soil background were not taken into account in examining the relationship between NDVI and vegetation cover. Using simulated AVHRR data derived from in situ spectral reflectance data which were collected from grasslands in Mongolia and Japan, Purevdorj et al. (1998) found a second-order polynomial best related NDVI to percent vegetation cover. Leprieur et al. (2000) found a curvilinear regression between the fractional vegetation cover and NDVI for a vegetation gradient in the south Sahel.

As the spatial resolution of satellite sensors varies from a few meters to several kilometers, and some models need input parameters from various data sources with different spatial resolutions, properly dealing with the spatial scale problem of satellite data is inevitable. In quantitative analysis of remote sensing, the relationship between surface property measurements at different spatial resolutions often causes concern (Chen, 1999). In order to compare NDVI at different spatial resolutions over the same surface, it is desirable to evaluate the impact of spatial resolution on the NDVI measurement. Since vegetation cover can be highly heterogeneous spatially, subpixel variability is likely to introduce uncertainties in the NDVI values at different resolutions.

Several studies have investigated the impact of spatial resolution on NDVI, but with conflicting results. Aman et al. (1992) analyzed the correspondence between NDVI calculated from average reflectances and NDVI integrated from individual NDVIs by simulating AVHRR data from high spatial resolution SPOT 1 HRV radiometer and Landsat Thematic Mapper (TM) data. For the study sites located in tropical West Africa and temperate France, a strong correlation was found between the two types of NDVI computed and they concluded that NDVI derived from the coarse spatial resolution sensor data can be used in lieu of NDVI integrated from fine spatial resolution without introducing significant errors. Wood and Lakshmi

(1993) showed the NDVI as scale invariant at the FIFE experiment site in Kansas, however, the relative homogeneity of the FIFE site prevented the generalization of this conclusion (Hu & Islam, 1997). On the other hand, Price (1992) noted that for a region consisting of a mixture of totally vegetated area and non-vegetated area, prominent discrepancies occur between NDVI derived from high resolution measurements and NDVI derived from low resolution measurements, with the relative difference approaching 30%. Hu and Islam (1997) agreed with Price, and they successfully parameterized subpixel scale heterogeneity effects on NDVI using simulated land and vegetation scenarios and by modeling the variances and covariance terms with the pixel scale values. The effects of scaling on the retrieval of LAI from NDVI based on NDVI–LAI relationships were investigated using mixed water-vegetation pixels, and large biases were found when pixels contain interfaces between two or more contrasting surfaces (Chen, 1999).

As the literature review above indicates, there exist many perspectives and discrepancies on the two related issues of the relationship between NDVI and fractional vegetation cover and the scale effect of NDVI. The principle behind derivation of fractional vegetation cover from NDVI is to relate NDVI of mixed pixels to reference NDVI values, such as the NDVIs of dense vegetation and bare soil, assuming the individual component NDVIs in mixed pixels can be represented by these reference NDVIs. However, even if component NDVIs can be estimated as the reference NDVI without error, there are still sources of uncertainty caused by the scale effect of NDVI in retrieving vegetation fraction from NDVI. NDVI of mixed pixels and that of the components in mixed pixels are not at the same spatial scale, as the former is at pixel scale, while the latter is at subpixel scale. It remains unclear the extent to which the pixel scale NDVI corresponds to the subpixel scale NDVI and what possible relationships exist between them. The relationship between NDVI and fractional vegetation cover appears to be directly influenced by the scale effect of NDVI and an understanding of this effect is essential to understanding the relationship between NDVI and fractional vegetation cover, and for accurate retrievals of vegetation fraction. There are few studies that have examined the relationship between NDVI and fractional vegetation cover taking into account of the scale effect of NDVI.

This paper has two objectives. The first is to analyze the difference between NDVI calculated from average reflectances, which represents NDVI derived from coarse spatial resolution data, and NDVI integrated from individual component NDVIs, which represents NDVI derived from fine spatial resolution data, over heterogeneous surfaces. The second is to examine the relationship between NDVI and fractional vegetation cover taking into account scaling effects and then propose a scale invariant method to derive fractional vegetation cover from red and NIR reflectances.

2. Review of methods to retrieve vegetation fraction from NDVI

There are three semi-empirical relationships used to derive vegetation fraction from NDVI. Baret et al. (1995) developed a generic semi-empirical relationship between the vertical gap fraction and vegetation index and proposed a method to derive vegetation fraction (f) from NDVI:

$$f = 1-\left(\frac{\mathrm{NDVI}_\infty-\mathrm{NDVI}}{\mathrm{NDVI}_\infty-\mathrm{NDVI}_S}\right)^{0.6175} \quad (2)$$

where NDVI_∞ and NDVI_S are the NDVI for vegetation with infinite LAI and bare soil, respectively. Based on a simple radiative transfer model, Carlson and Ripley (1997) proposed a semi-empirical relationship as follows:

$$f = \left(\frac{\mathrm{NDVI}-\mathrm{NDVI}_S}{\mathrm{NDVI}_\infty-\mathrm{NDVI}_S}\right)^2 \quad (3)$$

Using a *dense vegetation mosaic-pixel* model, Gutman and Ignatov (1998) assumed the NDVI of a mixed pixel can be represented as,

$$\mathrm{NDVI} = f\mathrm{NDVI}_\infty + (1-f)\mathrm{NDVI}_S \quad (4)$$

and the vegetation fraction derived by the scaled NDVI as,

$$f = \frac{\mathrm{NDVI}-\mathrm{NDVI}_S}{\mathrm{NDVI}_\infty-\mathrm{NDVI}_S} \quad (5)$$

3. Comparison of NDVI at different resolutions

3.1. Case I: A two-component scene model

When landscape components form large spatially coherent patches and the vertical dimension of the vegetation is small, spectral interactions between soil and vegetation components are negligible (Hanan et al., 1991), and the influence of the individual components on the observed reflectance can be described by their spectral properties and fractional area using a linear spectral mixing model (Adams et al., 1986; Gutman & Ignatov, 1998; Hanan et al., 1991; Small, 2001; Smith et al., 1990; Wittich & Hansing, 1995). Nonlinearity is introduced when multiple scattering of radiation occurs among the different target materials, a second-order effect that becomes dominant in the case of intimate mixtures (Clark & Lucey, 1984). In case I, we treat the landscape as composed of mixed pixels consisting of homogeneous vegetation patches and soil background, similar to the *dense vegetation mosaic-pixel* model proposed by Gutman and Ignatov (1998) (Fig. 1). Shadow components are assumed insignificant and negligible in this model. The red (R) and near infrared (N) reflectances of the mixed pixel are the area averaged reflectances of vegetation and soil (Manzi & Planton, 1994; Wittich & Hansing, 1995).

$$R = fR_V + (1-f)R_S \quad (6)$$

$$N = fN_V + (1-f)N_S \quad (7)$$

where f is vegetation fraction, and R_V and N_V are vegetation reflectances in red and NIR bands, respectively, and R_S and N_S are bare soil reflectances in red and NIR bands, respectively.

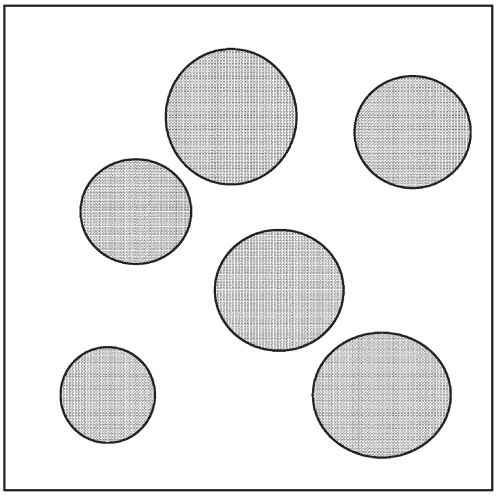

Fig. 1. Representation of mixed pixels in a landscape composed of homogeneous vegetation patches and soil background.

The NDVI of the mixed pixel or coarse resolution NDVI ($NDVI_C$) is

$$NDVI_C = \frac{N-R}{N+R} \tag{8}$$

If a hypothetical, finer resolution sensor were to measure the same landscape such that the NDVI of the two components could be resolved, then

$$NDVI_V = \frac{N_V-R_V}{N_V+R_V} \tag{9}$$

$$NDVI_S = \frac{N_S-R_S}{N_S+R_S} \tag{10}$$

The average NDVI of the coarse mixed pixel, as measured by the finer resolution $NDVI_F$ values is

$$NDVI_F = fNDVI_V + (1-f)NDVI_S \tag{11}$$

The $NDVI_F$ is a theoretical value which can be derived by infinite fine resolution data. The finer the resolution of a sensor, the lower the proportion of mixed pixels in the landscape, and the closer the average NDVI is to the theoretical value, $NDVI_F$. The definitions of fine and coarse resolution NDVI can be understood by comparing the resolution of sensors with the size of the elements in a landscape. Strahler et al. (1986) noted two discrete scene model possibilities, H- and L-resolution. In the H-resolution case, the resolution cells of the image are smaller than the elements, and the elements are individually resolved with $NDVI_F$ values. In the L-resolution case, the resolution cells are larger than the elements and they cannot be resolved (Strahler et al., 1986) with the coarse resolution, $NDVI_C$ values.

Differences between $NDVI_C$ and $NDVI_F$ are caused by the spatial scale of observations and the heterogeneity of the landscape. $NDVI_C$ is derived from the average reflectances of the entire pixel while $NDVI_F$ is an area weighted average of component NDVIs resolved by finer resolution sensors. If A denotes a weighted average function defined by Eqs. (6) and (7), V denotes the NDVI function defined by Eq. (1), and $\boldsymbol{X}$ is the vector of reflectances (R, N), then we can express NDVI as,

$$NDVI_C = V[A(\boldsymbol{X})] \tag{12}$$

$$NDVI_F = A[V(\boldsymbol{X})] \tag{13}$$

Thus, $NDVI_C$ and $NDVI_F$ are compounded by the same two functions, A and V, but with reversed sequences. Because V is a nonlinear function of reflectances and A is a linear function in terms of f, the inversion of the sequence of the two functions results in the difference between $NDVI_C$ and $NDVI_F$. If the equation of a vegetation index is a linear function of reflectances, it is scale invariant in accordance with Eqs. (12) and (13). Thus, the perpendicular vegetation index (PVI) (Richardson & Wiegand, 1977), the Tasseled cap green vegetation index (GVI) (Kauth & Thomas, 1976), the difference vegetation index (DVI) (Tucker, 1979) and weighted difference vegetation index (WDVI) (Clevers, 1989) are scale invariant if the linear mixture model holds true.

Finer resolution sensors can observe subpixel variations in a landscape, which are indistinguishable with coarser resolution sensors. In order to express $NDVI_F$ as the function of coarse resolution reflectances, N and R, the differences of red and NIR reflectances between vegetation and soil must be introduced,

$$\Delta N = N_V - N_S \tag{14}$$

$$\Delta R = R_V - R_S \tag{15}$$

In substituting ΔN, ΔR, N, and R for N_V, R_V, N_S, and R_S in Eq. (11), $NDVI_F$ can then be written as,

$$NDVI_F = \frac{N^2-R^2+A}{(N+R)^2+B} \tag{16}$$

$$A = (1-2f)(N-R)(\Delta N+\Delta R) - f(1-f)(\Delta N^2-\Delta R^2) \tag{16-1}$$

$$B = (1-2f)(N+R)(\Delta N+\Delta R) - f(1-f)(\Delta N+\Delta R)^2 \tag{16-2}$$

and $NDVI_C$ can be expressed similar to Eq. (16) as,

$$NDVI_C = \frac{N^2-R^2}{(N+R)^2} \tag{17}$$

Unlike the coarse resolution $NDVI_C$, the finer resolution $NDVI_F$ is determined not only by the average reflectances, but also by the subpixel variations (i.e. f, ΔN and ΔR). The difference between $NDVI_C$ and $NDVI_F$ is expressed by the two correction terms A and B, which cannot be obtained from the coarse resolution sensors and are thus neglected in $NDVI_C$.

It should be noted that the first terms of A and B (A_1 and B_1) do not contribute to the difference between $NDVI_C$ and $NDVI_F$, because

$$\frac{(1-2f)(N-R)(\Delta N+\Delta R)}{(1-2f)(N+R)(\Delta N+\Delta R)}=\frac{N-R}{N+R} \tag{18}$$

The ratio of the latter terms of A and B (A_2 and B_2),

$$\frac{-f(1-f)(\Delta N^2-\Delta R^2)}{-f(1-f)(\Delta N+\Delta R)^2}=\frac{\Delta N-\Delta R}{\Delta N+\Delta R}\neq\frac{N-R}{N+R} \tag{19}$$

however, explain the primary differences between $NDVI_C$ and $NDVI_F$.

When correction terms A_2 and B_2 become zero simultaneously, the difference between $NDVI_C$ and $NDVI_F$ become zero. There are three cases in which A_2 and B_2 are close to zero resulting in no scale influence on NDVI. First, when f is close to zero or one, which means that a mixed pixel is nearly homogenous spatially; second, when ΔN and ΔR are close to zero, which means that a mixed pixel is nearly homogeneous with respect to their spectral reflectances; and third, when $\Delta N+\ \Delta R$ is close to zero (i.e. N_V+R_V close to N_S+R_S), the difference between $NDVI_C$ and $NDVI_F$ become zero. Thus, for spatially and spectrally heterogeneous surfaces, NDVI is scale invariant only when the brightness of vegetation (brightness defined as the sum of red and NIR reflectances here) is equal to that of soil background. The brightness contrast between vegetation and soil background and vegetation fraction are two key factors that determine the scale effect of NDVI.

3.2. Case II: A three-component scene model

Shadows cast by vegetation canopies can be an important component of the total pixel reflectance, particularly when the ratio of canopy height to width is high. Shadows change not only with the position of the sun and the amount of diffuse solar radiation, but also with the density and geometric characteristics of vegetation canopies (Jasinski & Eagleson, 1989; Huemmrich, 2001). Li and Strahler (1986) and Jasinski (1996) described four-component geometrical models to estimate sunlit and shadowed canopy and soil areas of forest canopies. Huemmrich (2001) combined the SAIL model (Alexander, 1983; Verhoef, 1984) with the Jasinski geometric model (Jasinski, 1990a; Jasinski & Eagleson, 1989) to simulate canopy spectral reflectance and absorption of photosynthetically active radiation for discontinuous canopies. Their model was a three-component geometric model (sunlit canopy, sunlit soil, and shadowed soil), and was shown adequate to describe forest reflectances (Huemmrich (2001).

In case II, shadows cast by plants on soil were added as a component into the scene model of case I. This model assumes that canopies do not shadow and overlap each other; the size of the canopy elements is small relative to the size of pixels, and surface is observed from nadir. The fractional area of shadowed soil, g_{sh}, can be estimated as (Jasinski, 1990a):

$$g_{sh}=1-f-(1-f)^{\eta+1} \tag{20}$$

where η is a nondimensional solar-geometric similarity parameter defined as the ratio of the mean shadow area cast by a single plant to the mean projected canopy area (Jasinski, 1996). Analytical expressions for several geometrical shapes have been developed by Jasinski (1990b). The fractional area of illuminated soil background, g_l, can then be calculated by

$$g_l=1-f-g_{sh}=(1-f)^{\eta+1} \tag{21}$$

The red and NIR reflectances of the scene are the area weighted reflectances of the three components (illuminated canopy, sunlit soil and shadowed soil,)

$$R=fR_V+g_lR_S+g_{sh}R_{Sh} \tag{22}$$

$$N=fN_V+g_lN_S+g_{sh}N_{Sh} \tag{23}$$

where R_{Sh} and N_{Sh} are the red and NIR reflectances of shadowed soil, respectively. When sun zenith angle is 0 (i.e. $\eta=0$), the three-component scene model reduces to the two-component scene model.

The $NDVI_F$ of mixed pixels is

$$NDVI_F=f\,NDVI_V+g_l NDVI_S+g_{sh}NDVI_{Sh} \tag{24}$$

where $NDVI_{Sh}$ is the NDVI of shadowed soil component. By defining B_V, B_S, B_{Sh} as the brightness of vegetation canopy, illuminated soil, and shadowed soil components (e.g. $B_V=N_V+R_V$), the $NDVI_C$ can be expressed as:

$$NDVI_C=\frac{fB_V NDVI_V+g_lB_S NDVI_S+g_{sh}B_{Sh}NDVI_{Sh}}{fB_V+g_lB_S+g_{sh}B_{Sh}} \tag{25}$$

Eqs. (24) and (25) describe the relationship between pixel scale NDVIs and subpixel scale component NDVIs. The contribution of an individual component NDVI to the $NDVI_F$ is only determined by its fractional cover. However, the contribution of an individual component NDVI to the $NDVI_C$ is determined not only by its fractional cover, but also by its brightness. Eq. (25) also indicates that the $NDVI_C$ will not change linearly with changing of component fractional cover except when the brightness of all the components is equal. Bright components will have relatively greater influence on the $NDVI_C$. At low vegetation fractions, dark soil background will increase the contribution of the $NDVI_V$ to the $NDVI_C$ and result in overestimation of vegetation amounts. At high vegetation fractions, shadow dominating canopy background will bring the $NDVI_C$ close to the $NDVI_V$ even though the scene is not fully covered by the vegetation canopy.

Pixel scale NDVI cannot be calculated from subpixel scale NDVI without knowledge of the component brightness values of the mixed pixel. Uncertainty exists in Eq. (4) because of the scale effect of NDVI which is responsible for the difference between $NDVI_C$ and $NDVI_F$. Consequently, for heterogeneous surfaces, vegetation fraction cannot be accurately estimated from NDVI because of its spatial scale effect and nonlinear relationship with vegetation fraction.

4. Derivation of vegetation fraction from red and NIR reflectances

The most distinct spectral characteristic of green vegetation, different from that of bare soil, is the strong contrast between NIR and red reflectances, with very low red reflectance and high NIR reflectance. The difference between NIR and red reflectances of a mixed pixel can be obtained by combining Eqs. (22) and (23)

$$N-R = f(N_V-R_V) + g_l(N_S-R_S) + g_{Sh}(N_{Sh}-R_{Sh}) \quad (26)$$

Generally, the NIR reflectance of bare soil is slightly larger than red reflectance. The reflectance of shadowed soil is very low, but its NIR reflectance is slightly larger than red reflectance because of higher canopy transmittance in the NIR band than in red band. Fitzgerald et al. (2005) measured several spectra of dry soil shadowed by one leaf layer and found their NIR reflectances were about 0.06 and their red reflectance was about 0.02. By assuming that the difference between NIR and red reflectances of illuminated soil and that of shadowed soil are equal, Eq. (26) can be reduced to

$$N-R = f(N_V-R_V) + (1-f)(N_S-R_S) \quad (27)$$

Thus vegetation fraction can be derived from the red and NIR reflectances according to

$$f = \frac{N-R-(N_S-R_S)}{N_v-R_v-(N_S-R_S)} \quad (28)$$

Since the difference vegetation index (DVI) is defined as the difference between the NIR and red reflectances ($N-R$), Eq. (28) can be considered as a scaled difference vegetation index (SDVI) between bare soil DVI, (DVI_S) and dense vegetation DVI (DVI_V),

$$SDVI = \frac{DVI-DVI_S}{DVI_V-DVI_S} \quad (29)$$

In this case, SDVI is equal to f in value and thus can be used directly as a vegetation fraction index. Fig. 2 shows the isolines of SDVI. Adjacent isolines are parallel and equidistant, and the slope of the soil line is assumed as 1 by SDVI. SDVI is 0 on the soil line and SDVI becomes 1 for dense vegetation. For a mixed pixel, SDVI and f are calculated according to the distance between a point corresponding to the pixel and the soil line in red-NIR space.

Eq. (26) indicates that, unlike the NDVI, the DVI is insensitive to the variation of fractional cover of shadowed soil since the DVI value of shadowed soil is often very small.

Soil background spectra are widely variable with variations in soil biogeochemical constituents, moisture and roughness. The soil reflectance at one band is often functionally related to the reflectance at another band, and the reflectances of various soils would fall on a straight line, called a soil line, in spectral space. Orthogonal vegetation indices, including the PVI, GVI and DVI, were developed based on the concept that a vegetation point would deviate from the soil line with the perpendicular distance from the point to the soil line being a measure of the amount of vegetation present (Jackson, 1983). Other orthogonal vegetation indices instead of the DVI could be applied in Eq. (29). Price (1992) proposed that the vegetation fraction of a mixed pixel can be derived by the ratio of the PVI of the pixel to dense vegetation PVI, which differs from SDVI only in the slope of the soil line in that DVI assumes it equal to 1. Raffy et al. (2003) and Raffy and Soudani (2004) reported that the percentage of forest cover could be accurately estimated by a scaled PVI when the local LAI of a forest varies slightly.

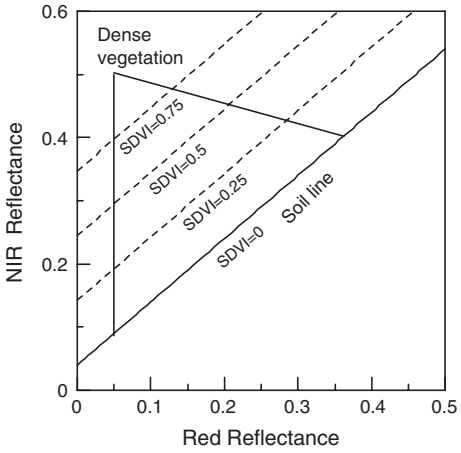

Fig. 2. Isolines of SDVI for estimation of vegetation fraction.

5. Results

5.1. NDVIs at different resolutions

Following Carlson and Ripley (1997), the red and NIR reflectances of soil background in the mixed pixel (Fig. 1) were set at 0.08 and 0.11, respectively, and those of vegetation patches were set at 0.05 and 0.50, respectively. The shadow component was included in the three-component scene model by setting η at 1. The two-component scene model is a special case of the three-component scene model when η is 0. The NIR and red reflectances of shadowed soil were assumed 0.06 and 0.02, respectively, and the $NDVI_{Sh}$ is 0.5. When $\eta=0$, $NDVI_F$ varies linearly with the variation of fractional vegetation cover, but $NDVI_C$ yields an upward-convex curve as the vegetation cover changes (Fig. 3a). The difference between $NDVI_C$ and $NDVI_F$ is significant in this case. Since they are measurements of the same heterogeneous landscape, the resolution of measurements is responsible for the difference between them. The average ΔNDVI ($NDVI_C$ minus $NDVI_F$) is 0.107 over the entire range of vegetation fraction covers with a maximum ΔNDVI of 0.171 at a vegetation fraction of 0.35. When $\eta=1$, both $NDVI_C$ and $NDVI_F$ are increased in comparison with the corresponding $NDVI_C$ and $NDVI_F$ with $\eta=0$. The average ΔNDVI is 0.089 over the entire range of vegetation fraction covers.

If the red and NIR reflectances of soil background are set at 0.18 and 0.23, respectively, the difference between $NDVI_C$ and

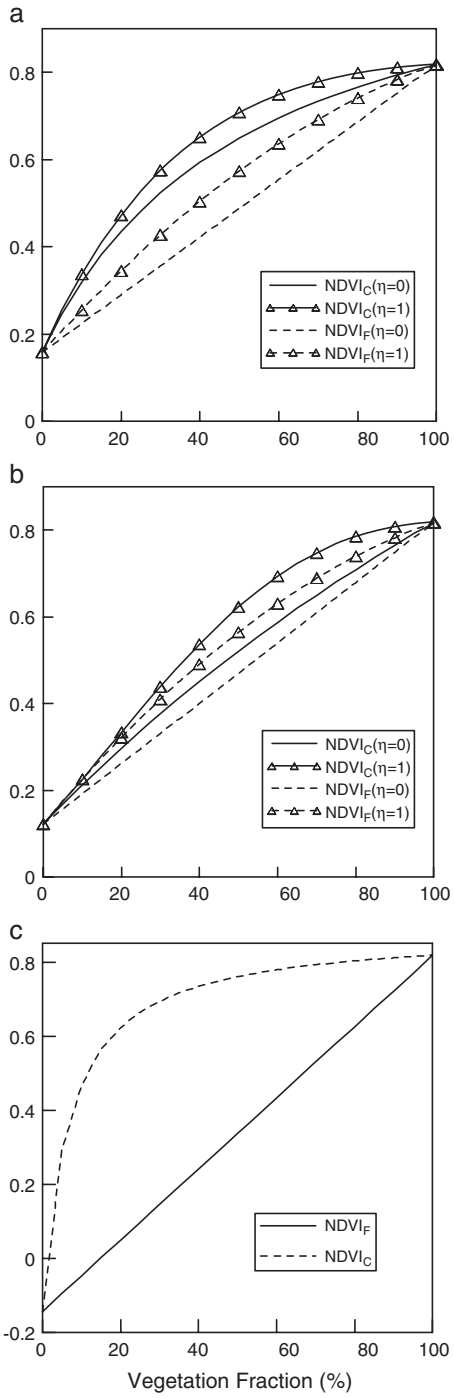

Fig. 3. NDVI of a mixed vegetation-soil (water) landscape at fine and coarse resolutions versus fractional vegetation cover, N_V=0.5, R_V=0.05, N_{Sh}=0.06, R_{Sh}=0.02, (a) N_S=0.11, R_S=0.08. (b) N_S=0.23, R_S=0.18. (c) R_W=0.02, N_W=0.015 (shadow was neglected).

$NDVI_F$ is insignificant (Fig. 3b). When η=0, $NDVI_C$ is close to $NDVI_F$ at any fractional vegetation cover. The average ΔNDVI is 0.032 over all vegetation fractions and ΔNDVI reaches a maximum of 0.051 at a vegetation fraction of 0.45 for this case. When η=1, both $NDVI_C$ and $NDVI_F$ are increased, particularly at high vegetation fractions, in comparison with the corresponding $NDVI_C$ and $NDVI_F$ with η=0. The average ΔNDVI is the same as that with η=0, but ΔNDVI reaches a maximum of 0.063 at a vegetation fraction of 0.60 for this case. Thus, the nonlinearity of $NDVI_C$ becomes prominent not only with the darkening of soil background, but also with the presence of shadow. We can conclude that the presence of shadow in partially vegetated surfaces will result in overestimation of NDVI and vegetation amounts in mixed pixels, as well as result in saturation at high vegetation fractions.

In the case of mixed, vegetation-water landscapes, the difference between $NDVI_C$ and $NDVI_F$ is extreme (Fig. 3c). The red and NIR reflectances of water are assumed at 0.02 and 0.015, respectively, with vegetation reflectances the same as above. Shadow on water surfaces was negligible for very low reflectances of water. $NDVI_C$ is far larger than $NDVI_F$ and throughout most vegetation fractions the nonlinearity of $NDVI_C$ with vegetation fraction is particularly strong. When vegetation fraction is 0.15, $NDVI_C$ is 0.56 even though the value of $NDVI_F$ is only zero. $NDVI_C$ cannot truly approximate the presence of vegetation in this case. There is a large bias in NDVI values at different resolutions in landscapes containing vegetation and open water. Chen (1999) similarly found large biases in LAI, which is retrieved by using a NDVI–LAI relationship at

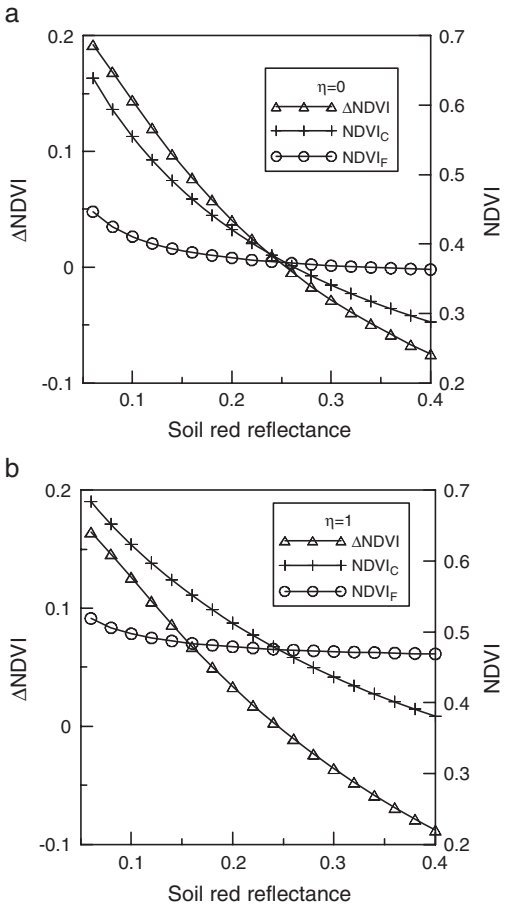

Fig. 4. Relationship between soil background red reflectance and NDVIs at fine and coarse resolutions, and the difference between them (ΔNDVI) for the case of vegetation fraction=0.4, vegetation reflectances as in Fig. 3, and soil line of y=1.062×+0.026 (Huete et al., 1985). (a) η=0; (b) η=1.

different resolutions in boreal forest–water mixed landscapes. These biases are introduced by resolution-dependent differences between $NDVI_C$ and $NDVI_F$.

If the fractional vegetation cover is fixed at 0.4 and the reflectances of vegetation are assumed as above, ΔNDVI becomes a function of soil background reflectances. If a soil line is assumed, as measured by Huete et al. (1985), ΔNDVI changes with variations of soil red reflectance (Fig. 4). When $\eta=0$, $NDVI_F$ changes very little with the variation of soil red reflectance, and this small change is due to the variation of NDVI of the soil component, which changes from 0.19 for dark soil to 0.06 for bright soil. But $NDVI_C$ changes dramatically with variations in soil red reflectance, from 0.63 for dark soil background to 0.32 for bright soil background. ΔNDVI is large when soil background is dark and it becomes small and negative when soil red reflectance is larger than 0.26. In case of $\eta=1$, ΔNDVI, $NDVI_C$ and $NDVI_F$ behave similar to those without shadow, but $NDVI_C$ and $NDVI_F$ are increased in comparison with those without shadow, particularly over bright soil backgrounds. This demonstrates that the measurement spatial

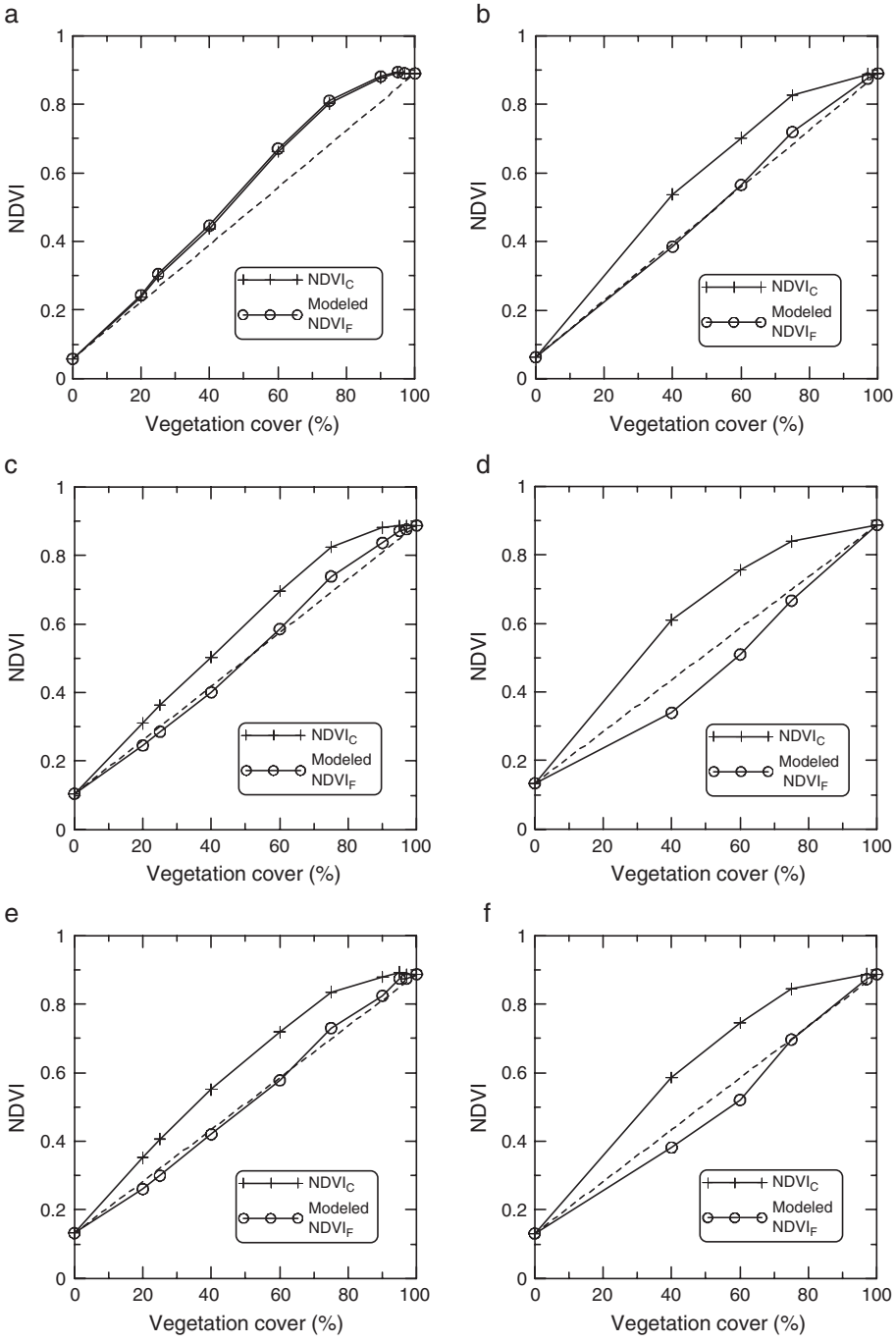

Fig. 5. Comparison of modeled $NDVI_F$ with theoretical $NDVI_F$. (a) Superstition sand (dry). (b) Superstition sand (wet). (c) Avondale loam (dry). (d) Avondale loam (wet). (e) Whitehouse-B sandy clay loam (dry). (f) Whitehouse-B sandy clay loam (wet).

Table 1
Comparison of the deviations of $NDVI_C$ and $NDVI_F$ from theoretical $NDVI_F$

Soil	Soil red reflectance	No. of Points	$NDVI_C$ mean deviation	$NDVI_F$ mean deviation
Superstition (Dry)	0.337	8	0.0574	0.0626
Avondale loam (Dry)	0.188	8	0.0793	0.0211
Superstition (Wet)	0.187	4	0.1131	0.0152
Whitehouse (Dry)	0.158	8	0.0843	0.0180
Whitehouse (Wet)	0.126	4	0.1206	0.0316
Avondale loam (Wet)	0.107	3	0.1616	0.0683
Total		35	0.0896	0.0344

resolution makes a significant difference in NDVI values computed over heterogeneous landscapes with and without shadows.

The $NDVI_C$ and $NDVI_F$ are two extreme cases of NDVI over heterogeneous surfaces. When scaling down from coarse resolution to fine resolution, the NDVI of a heterogeneous landscape would change monotonously from $NDVI_C$ to $NDVI_F$, because the heterogeneity within pixels would decrease at the scaling-down process until no mixed pixels exist, i.e. no heterogeneity existing within pixels.

5.2. Correcting coarse resolution NDVI to fine resolution NDVI using experimental data

As demonstrated in Fig. 3, the NDVI of a mixed pixel does not vary linearly with fractional vegetation cover, so it cannot quantify the amount of vegetation accurately. However, NDVI derived from a hypothetical fine resolution sensor, $NDVI_F$, does vary linearly with fractional vegetation cover according to the two-component scene model. In this section, we use experimental data from Huete et al. (1985) to examine the usefulness of Eq. (16) to correct coarse resolution NDVI to fine resolution NDVI.

Huete et al. (1985) measured the reflectances of a developing cotton canopy in red (0.63~0.69 μm) and NIR (0.76~0.90 μm) bands over four different soil backgrounds in dry and wet condition and for six different green cover levels. The theoretical $NDVI_F$ of a landscape composed of two homogeneous components is calculated by the straight line interpolation of component NDVIs using fractional vegetation cover (Eq. (11)).

Solar zenith angle variations along with cotton canopy development through the growing season, result in complex shadow component variations that are difficult to quantify. For simplicity, the shadow effects were not taken into account in the correction. Estimates of expected $NDVI_F$ were calculated using Eq. (16) with prior knowledge of fractional vegetation cover and red and NIR reflectance differences between components (vegetation and soil), but without knowledge of the red and near-infrared reflectances (Fig. 5). The modeled $NDVI_F$ values for various soil backgrounds corresponded fairly closely to the theoretical $NDVI_F$, suggesting that the two-component scene model could explain the nonlinearity of NDVI in most cases. For dry Superstition sand, which is brighter than the other soils, modeled $NDVI_F$ was not as close to the theoretical $NDVI_F$ as $NDVI_C$ (Fig. 5a). This was possibly caused by shadow effects since shadows dominate soil background when vegetation fraction is high and the bright soil is darkened by shadow. The shape of the NDVI-f curve in this case is similar to that of the $NDVI_C$-f curve with $\eta=1$ in Fig. 3b, i.e. NDVI increases linearly at low vegetation fractions and becomes saturated at

Table 2
Mean errors of the four methods used to derive vegetation fraction over each soil background

Soil	Dry/ wet	No. of points	R_S	SDVI (%)	Gutman and Ignatov (%)	Carlson and Ripley (%)	Baret et al. (%)
Superstition	D	8	0.337	2.65	6.90	9.84	4.26
	W	4	0.187	5.23	13.67	5.00	1.41
Avondale	D	8	0.188	4.17	9.32	8.69	3.28
	W	3	0.107	8.39	21.44	6.91	6.22
Whitehouse	D	8	0.158	4.83	11.10	7.70	2.15
	W	4	0.126	7.22	15.94	6.74	5.22
Cloversprings	D	8	0.062	7.51	17.01	6.64	7.29
	W	5	0.029	8.55	26.14	15.54	17.93
Total		48		5.65	13.92	8.51	5.64

R_S is the red reflectance of soil background.

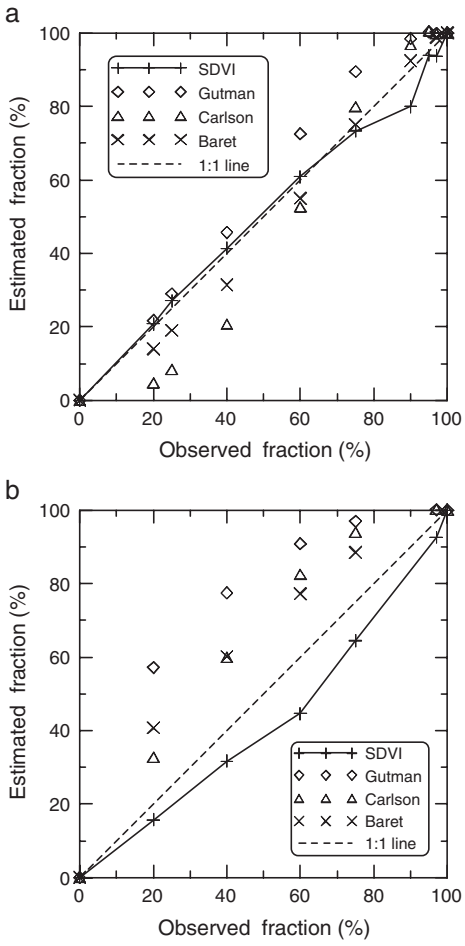

Fig. 6. Comparison of observed fractions and estimated fractions using the four different methods over individual soil backgrounds (a) over dry Superstition sand (bright) background. (b) Wet Cloversprings loam (dark) background.

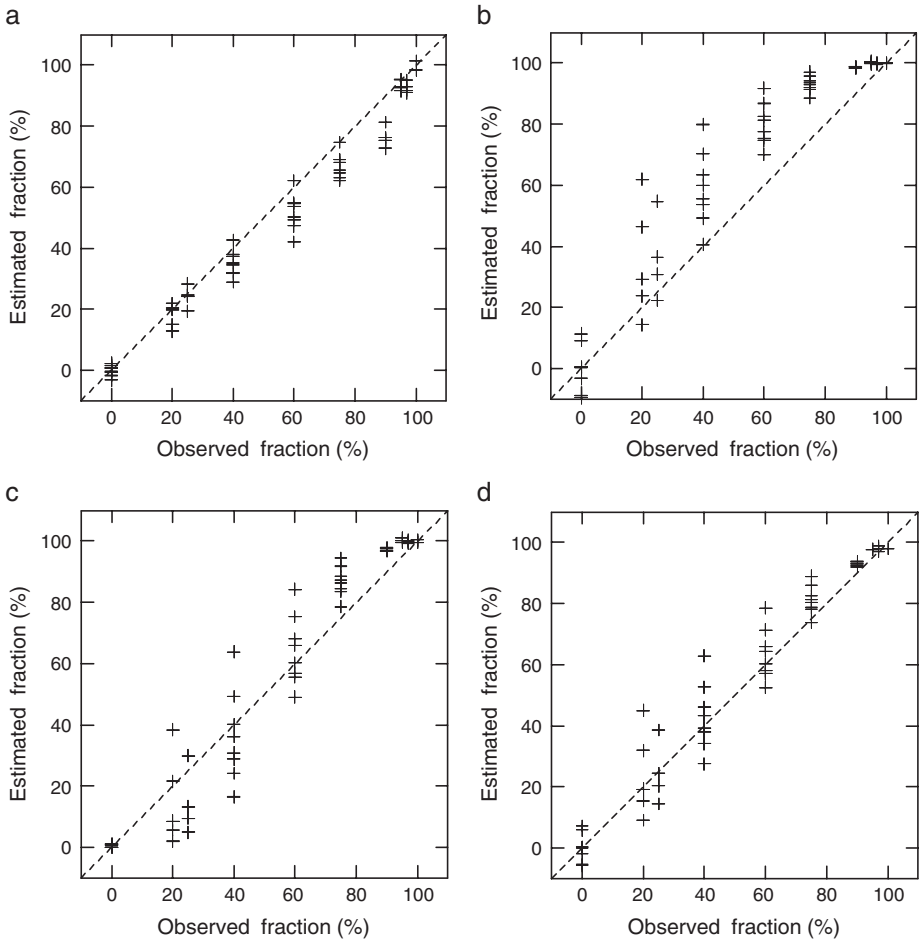

Fig. 7. Comparison of observed vegetation and estimated vegetation fractions using different methods over various soil backgrounds. (a) SDVI. (b) Gutman and Ignatov's method. (c) Carlson and Ripley's method. (d) Method by Baret et al.

high vegetation fractions, indicating the shadow effects are mostly responsible for the nonlinearity of NDVI over bright soil backgrounds. The correction of NDVI for the mixed pixel with Cloversprings loam background which is very dark ($R_S \leq 0.062$) was unsuccessful, which may be a result of the numerator and denominator of $NDVI_F$ (Eq. (16)) being so small that slight changes in reflectance from the linearity assumption could cause great error in $NDVI_F$ estimation.

The total mean deviation of modeled $NDVI_F$ from theoretical $NDVI_F$ is 0.0344, which is much smaller than the mean deviation of $NDVI_C$, 0.0896 (Table 1). The deviation of modeled $NDVI_F$ is mostly caused by the shadow effects. The relatively big deviation of $NDVI_C$ can be mostly explained by the scale effect of NDVI, as dark soil backgrounds correspond to big deviations of $NDVI_C$, and except for the dry Whitehouse loam, the darker the soil background is, the bigger the deviation of $NDVI_C$.

5.3. Validation of the SDVI as a vegetation fraction index

The experimental data measured by Huete et al. (1985) was used to validate Eq. (28) and estimate the accuracy of SDVI as a vegetation fraction index. Three methods reviewed above that derive vegetation fraction from NDVI were also evaluated and compared to the proposed method. First, the performances of the four methods were evaluated and compared using specific soil backgrounds. $NDVI_S$ and $NDVI_V$ were given by NDVI for bare soil and fully covered vegetation, respectively. At 100% green cover, only the dark Cloversprings loam and bright Superstition sand were used as soil background since the soil background influence is negligible in the red and very small in the NIR (0.017) for the dense vegetation (Huete et al., 1985). The mean errors, calculated by the mean deviations of derived fraction from observed fraction, of the four methods are summarized in Table 2. The total mean error of SDVI was the lowest and was approximately the same as the method of Baret et al. (1995). The method of Gutman and Ignatov (1998) produced

Table 3
Evaluation of different methods to derive vegetation fraction

Methods	Mean error (%)	RMSD (%)	Standard deviation (%)	Bias (%)
SDVI	5.42	7.11	5.25	−4.79
Gutman and Ignatov	12.82	16.34	11.38	11.72
Carson and Ripley	8.11	10.63	10.47	1.81
Baret et al.	6.00	8.28	7.80	2.73

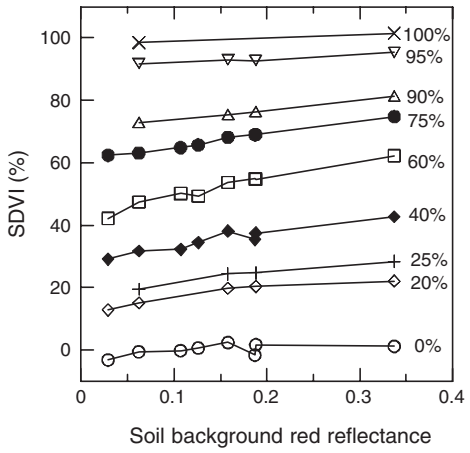

Fig. 8. Relationship between the SDVI and bare soil red reflectance for various vegetation fractions. The data is from Huete et al. (1985).

the biggest error, particularly with dark soil backgrounds (Fig. 6b). The mean error of the method of Carlson and Ripley (1997) was intermediate, but significant for the darkest soil background. The mean error of the method by Baret et al. is small except for over the darkest soil background. All the three NDVI based methods produced large error over dark soil background, and by contrast the SDVI performed fairly well over all soil backgrounds (Fig. 6).

The four methods were also evaluated over all the soil backgrounds (Fig. 7 and Table 3). The R_S, N_S and $NDVI_S$ were given by the average red, NIR reflectances, and NDVI of all the bare soil backgrounds, respectively, and the R_V, N_V and $NDVI_V$ were given by the average red, NIR reflectances, and NDVI of vegetation at 100% cover, respectively. SDVI performed best over the four methods with the estimated fraction close to the observed fraction over all percent vegetation covers with various soil backgrounds (Fig. 7a). The mean error and root mean square deviation (RMSD) of SDVI were least, 5.42% and 7.11% (Table 3), respectively. The low standard deviation results of SDVI indicated that variation of soil backgrounds produced the smallest influence on SDVI and that SDVI was robust enough to derive vegetation fraction over a wide range of soil background conditions. The bias of SDVI was −4.79%, indicating that the method slightly underestimated vegetation fraction. The bias can be largely explained by a nonlinear increase in NIR reflectance beyond 90% green cover, which was attributable to rapidly accumulating green biomass with only gradual lateral percent cover increase (Huete et al., 1985).

Large errors were brought out by Gutman and Ignatov's method with mean error and RMSD of 12.82% and 16.34%, respectively. The estimated fractions were 11.72% larger than the observed fractions on average, indicated by its bias, which can be largely explained by the scale effect of NDVI. When soil background is dark, the subpixel scale NDVI of the vegetation component has more influence on the pixel scale NDVI, which causes scaled NDVI to overestimate vegetation fraction. The large standard deviation of this method indicated that great uncertainty is introduced by soil background variations using this method. The mean error and RMSE were intermediate in Carlson and Ripley's method and were further reduced by the method of Baret et al. Mean biases were dramatically reduced by the latter two methods. In fact, these two methods transform scaled NDVI through power functions, which can produce negative modifications on scaled NDVI, and subsequently reduce the positive bias of the scaled NDVI. However, the transformation process removed only small uncertainties in NDVI caused by the variation of soil background. Thus, the standard deviations of these two methods were relatively large.

Although the method by Baret et al. performed slightly better than SDVI using individual soil backgrounds, SDVI outperformed this method over the various soil backgrounds, which demonstrated that the method by Baret et al. only performs better when soil background is invariant and its reflectances are given. The SDVI performed better over global soil background conditions, without knowledge of individual soil reflectances.

6. Discussion

Based on the assumption that the reflectances of a pixel composed of homogeneous vegetation, illuminated and shadowed soil can be calculated by area weighted averages of component reflectances, the difference between NDVI of a mixed pixel calculated at pixel scale, $NDVI_C$, and NDVI integrated by component NDVIs at the subpixel scale, $NDVI_F$, was analyzed. Analytical results showed that they are different in formulation. It is suggested that for heterogeneous surfaces, spatial resolution has an important impact on NDVI measurement and NDVI at different scales may not be comparable.

The nonlinearity of $NDVI_C$ becomes prominent not only with the darkening of soil background, but also with the presence of shadow. Even if the reflectances of a mixed pixel can be described by a linear mixing model, the NDVI of a mixed pixel cannot be calculated by the area weighted average of component NDVIs. Vegetation fraction should not be estimated by the scaled NDVI taken between the bare soil NDVI and dense vegetation NDVI, which would overestimate vegetation fraction in most cases. The proper linear relationship between NDVI and fractional vegetation cover is not reproduced by a coarse resolution sensor which acquires, with a single measurement, the vegetation index of an area of mixed cover, and thus NDVI does not have a unique correlation with vegetation cover (Price, 1990). The power function transformations of the scaled NDVI may improve the accuracy of vegetation estimation to a certain extent, but they cannot reduce the uncertainty in NDVI caused by the variation of soil backgrounds. The NDVI is an ad hoc prescription with no explicit physical relationship to vegetation measures such as LAI and vegetation fraction (Price & Bausch, 1995), It infers the presence of vegetation on the basis of the ratio of NIR reflectance to red reflectance, but does not provide areal estimations of the amount of vegetation (Small, 2001). Small (2001) found that the NDVI obtained from Landsat TM becomes asymptotic above intermediate vegetation fractions in much the same manner that it saturates with increased values of LAI and overestimates the abundance of interspersed vegetation relative to more densely

vegetated areas. This phenomenon may be partly due to the shadow effects on the NDVI.

The vegetation fraction of a mixed pixel can be estimated by a linear function of red and NIR reflectances, SDVI, which is scale invariant. This method of estimating vegetation fraction was validated by the experimental data acquired by Huete et al. (1985). Although soil and plant spectra interactively mix in a nonadditive, partly correlated manner to produce composite canopy spectra, the estimated vegetation fractions are fairly close to the observed fractions, which suggest SDVI being a robust index to derive vegetation fraction from red and NIR reflectances.

The variation of soil background brightness introduced relatively insignificant variation in SDVI at a constant vegetation cover, and SDVI is almost directly proportional to fractional vegetation cover (Fig. 8). The linearity of SDVI ensures that it outperforms NDVI to estimate vegetation fraction. Compared with other vegetation indices, Díaz and Blackburn (2003) found the difference vegetation index (DVI) to be the optimal vegetation index for estimating the biophysical properties of mangroves with various soil backgrounds because it has a robust linear relationship with LAI and percent cover.

Many vegetation indices are used to estimate vegetation fraction. However, a vegetation index compresses the volume of remote sensing data by a factor equal to the number of channels used, and significantly reduces the information contained in the original data set (Verstraete et al., 1996). The choice among vegetation indices to be used to infer vegetation fraction is crucial to the accuracy of estimation. The results of this study suggest that SDVI is an appropriate index to infer vegetation fraction of partially vegetation surfaces to the extent that the assumption of spectral mixture linearity holds. The extension of this approach to more complicated vegetation canopies (e.g. forests) remains to be analyzed. As other orthogonal vegetation indices, SDVI does not take into account the differential canopy transmittances in red and NIR wavelengths and nonlinear spectral mixing of soil and vegetation components. Both linear relationships with a biophysical parameter, e.g. vegetation fraction or LAI, and nonlinear spectral mixtures of landscape components should be considered and balanced in an optimal manner in future studies to develop an ideal vegetation index.

It should be noted that our analysis and validation were both based on ground surface reflectances. Atmospheric effects were not considered and evaluated in this study, and remain to be studied. Atmospheric correction thus may be necessary before using SDVI to derived vegetation fraction. Further validation based on satellite data with coincident field measurements over various landscapes would further provide meaningful results and be beneficial to assess the general applicability of SDVI as a vegetation fraction index.

Acknowledgements

This work was supported by the Natural Science Foundation of China (40201036) and the Project of the Ministry of Education on Doctoral Discipline of China (20030027014). We thank two anonymous reviewers for their helpful comments on the earlier version of the manuscript.

References

Adams, J. B., Smith, M. O., & Johnson, P. E. (1986). Spectral mixture modelling: A new analysis of rock and soil types at the Viking Lander 1 site. *Journal of Geophysical Research*, *91*, 8089–9012.

Alexander, L. (1983). SAIL canopy model FORTRAN software. Lyndon B. Johnson space center, NASA technical report JSC-18899.

Aman, A., Randriamanantena, H. P., Podaire, A., & Froutin, R. (1992). Upscale integration of normalized difference vegetation index: The problem of spatial heterogeneity. *IEEE Transactions on Geoscience and Remote Sensing*, *30*, 326–338.

Baret, F., Clevers, J. G. P. W., & Steven, M. D. (1995). The robustness of canopy gap fraction estimations from red and near-infrared reflectances: A comparison of approaches. *Remote Sensing of Environment*, *54*, 141–151.

Carlson, T. N., & Ripley, D. A. (1997). On the relation between NDVI, fractional vegetation cover, and leaf area index. *Remote Sensing of Environment*, *62*, 241–252.

Chen, J. (1999). Spatial scaling of a remotely sensed surface parameter by contexture. *Remote Sensing of Environment*, *69*, 30–42.

Choudhury, B. J., Ahmed, N. M., Idso, S. B., Reginato, R. J., & Daughtry, C. S. T. (1994). Relations between evaporation coefficients and vegetation indices studied by model simulations. *Remote Sensing of Environment*, *50*, 1–17.

Clark, R. N., & Lucey, P. G. (1984). Spectral properties of ice-particulate mixtures and implications for remote sensing 1. Intimate mixtures. *Journal of Geophysical Research*, *89*, 6341–6348.

Clevers, J. G. P. W. (1989). The application of a weighted infrared-red vegetation index for estimating leaf area index by correction for soil moisture. *Remote Sensing of Environment*, *29*, 25–37.

Colwell, J. E. (1974). Vegetation canopy reflectance. *Remote Sensing of Environment*, *3*, 175–183.

Curran, P. J. (1983). Multispectral remote sensing for the estimation of green leaf area index. *Philosophical Transactions of the Royal Society of London, Series A: Mathematical and Physical Sciences*, *309*, 257–270.

Díaz, B. M., & Blackburn, G. A. (2003). Remote sensing of mangrove biophysical properties: From a laboratory simulation of the possible effects of background variation on spectral vegetation indices. *International Journal of Remote Sensing*, *24*, 53–73.

Dymond, J. R., Stephens, P. F., & Wilde, R. H. (1992). Percentage vegetation cover of a degrading rangeland from SPOT. *International Journal of Remote Sensing*, *13*(11), 1999–2007.

Elvidge, C. D., & Chen, Z. (1995). Comparison of broad-band and narrow-band red and near-infrared vegetation indices. *Remote Sensing of Environment*, *54*, 38–48.

Fitzgerald, G. J., Pinter, P. J., Hunsaker, D. J., & Clarke, T. R. (2005). Multiple shadow fractions in spectral mixture analysis of a cotton canopy. *Remote Sensing of Environment*, *97*, 526–539.

Gillies, R. R., & Carlson, T. N. (1995). Thermal remote sensing of surface soil water content with partial vegetation cover for incorporation into climate models. *Journal of Applied Meteorology*, *34*, 745–756.

Gutman, G., & Ignatov, A. (1998). The derivation of the green vegetation fraction from NOAA/AVHRR data for use in numerical weather prediction models. *International Journal of Remote sensing*, *19*, 1533–1543.

Hanan, N. P., Prince, S. D., & Hiernaux, P. H. Y. (1991). Spectral modeling of multicomponent landscapes in the Sahel. *International Journal of Remote Sensing*, *12*, 1243–1258.

Hu, Z., & Islam, S. (1997). A framework for analyzing and designing scale invariant remote sensing algorithms. *IEEE Transactions on Geoscience and Remote Sensing*, *35*, 747–755.

Huemmrich, K. F. (2001). The GeoSail model: A simple addition to the SAVIL model to describe discontinuous reflectance. *Remote Sensing of Environment*, *75*, 423–431.

Huete, A. R. (1988). A soil-adjusted vegetation index (SAVI). *Remote Sensing of Environment*, *25*, 295–309.

Huete, A. R., & Liu, H. (1994). An error and sensitivity analysis of the atmospheric- and soil-correcting variants of the NDVI for the MODIS-EOS. *IEEE Transactions on Geoscience and Remote Sensing*, *32*, 897−905.

Huete, A. R., Jackson, R. D., & Post, D. F. (1985). Spectral response of a plant canopy with different soil backgrounds. *Remote Sensing of Environment*, *17*, 37−53.

Huete, A. R., Liu, H., & Leeuwen, W. V. (1997). A comparison of vegetation indices over a global set of TM images for EOS-MODIS. *Remote Sensing of Environment*, *59*, 440−451.

Jackson, R. D. (1983). Spectral indices in n-space. *Remote Sensing of Environment*, *13*, 409−421.

Jasinski, M. F. (1990a). Estimation of subpixel vegetation cover using red-infrared scattergrams. *IEEE Transactions on Geoscience and Remote Sensing*, *28*, 253−267.

Jasinski, M. F. (1990b). Functional relation among subpixel canopy cover, ground shadow, and illuminated ground at large sampling scales. *Proc. SPIE technical conf. remote sensing of the biosphere, Orlando, FL, 1300* (pp. 48−58).

Jasinski, M. F. (1996). Estimation of subpixel vegetation density of natural regions using satellite multispectral imagery. *IEEE Transactions on Geoscience and Remote Sensing*, *34*, 804−813.

Jasinski, M. F., & Eagleson, P. S. (1989). The structure of red-infrared scattergrams of semivegetated landscapes. *IEEE Transactions on Geoscience and Remote Sensing*, *27*, 441−451.

Kaufman, Y. J., & Tanré, D. (1992). Atmospherically resistant vegetation index (ARVI) for EOS-MODIS. *IEEE Transactions on Geoscience and Remote Sensing*, *30*, 261−270.

Kauth, R. J., & Thomas, G. S. (1976). The Tasseled Cap-a graphic description of the spectral-temporal development of agricultural crops as seen by Landsat. *Proc. Symp. on machine processing of remotely sensed data* (pp. 41−51). West Lafayette: Purdue University.

Kustas, W. P., Schmugge, T. J., Humes, K. S., Jackson, T. H., Parry, R., Weltz, M. A., et al. (1993). Relationships between evaporative fraction and remotely sensed vegetation index and microwave brightness temperature for semiarid rangelands. *Journal of Applied Meteorology*, *32*, 1781−1790.

Leprieur, C., Kerr, Y. H., Mastorchio, S., & Meunier, J. C. (2000). Monitoring vegetation cover across semi-arid regions: Comparison of remote observations from various scales. *International Journal of Remote Sensing*, *21*, 281−300.

Li, X., & Strahler, A. (1986). Geometric-optical bidirectional reflectance modeling of a conifer forest canopy. *IEEE Transactions on Geoscience and Remote Sensing*, *24*, 906−919.

Liu, H., & Huete, A. R. (1995). A feedback based modification of the NDVI to minimize canopy background and atmospheric noise. *IEEE Transactions on Geoscience and Remote Sensing*, *33*, 457−465.

Manzi, A. O., & Planton, S. (1994). Implementation of the ISBA parameterization scheme for land surface processes in a GCM—an annual cycle experiment. *Journal of Hydrology*, *155*, 353−387.

McDonald, A. J., Gemmell, F. M., & Lewis, P. E. (1998). Investigation of the utility of spectral vegetation indices for determining information on coniferous forests. *Remote Sensing of Environment*, *66*, 250−272.

Ormsby, J. P., Choudhury, B. J., & Owe, M. (1987). Vegetation spatial variability and its effect on vegetation indices. *International Journal of Remote Sensing*, *8*, 1301−1306.

Phulpin, T., Noilhan, J., & Stoll, M. (1990). Parameters estimates of a soil vegetation model using AVHRR data. *Proceedings of the 4th AVHRR data users meeting, Rothenburg, Germany, 5–8 Sept. 1989* (pp. 125−129). Darmstadt: EUMETSAT EUM P 06.

Price, J. C. (1990). Using spatial context in satellite data to infer regional scale evapotranspiration. *IEEE Transactions on Geoscience and Remote Sensing*, *28*, 940−948.

Price, J. C. (1992). Estimating vegetation amount from visible and near infrared reflectances. *Remote Sensing of Environment*, *41*, 29−34.

Price, J. C., & Bausch, W. C. (1995). Leaf area index estimation from visible and near-infrared reflectance data. *Remote Sensing of Environment*, *52*, 55−65.

Purevdorj, T., Tateishi, R., Ishiyama, T., & Honda, Y. (1998). Relationships between percent vegetation cover and vegetation indices. *International Journal of Remote Sensing*, *19*, 3519−3535.

Raffy, M., & Soudani, K. (2004). On the LAI of mixed soils–forests regions. *International Journal of Biometeorology*, *25*, 3073−3090.

Raffy, M., Soudani, K., & Trautmann, J. (2003). On the variability of the LAI of homogeneous covers with respect to the surface size and application. *International Journal of Biometeorology*, *24*, 2017−2035.

Richardson, A. J., & Wiegand, C. L. (1977). Distinguishing vegetation from soil background information. *Photogrammetric Engineering and Remote Sensing*, *43*, 1541−1552.

Rouse, J. W., Hass, R. H., Schell, J. A., & Deering, D. W. (1973). Monitoring vegetation systems in the Great Plains with ERTS. *Proceedings of the third ERTS symposium, Goddard Space Flight Center, December 1973, NASA SP-351* (pp. 309−317). Washington, DC: NASA.

Small, C. (2001). Estimation of urban vegetation abundance by spectral mixture analysis. *International Journal of Remote Sensing*, *22*, 1305−1334.

Smith, M. O., Ustin, S. L., Adams, J. B., & Gillespie, A. R. (1990). Vegetation in deserts: I. A regional measure of abundance from multispectral images. *Remote Sensing of Environment*, *31*, 1−26.

Strahler, A. H., Woodcock, C. E., & Smith, J. A. (1986). On the nature of models in remote sensing. *Remote Sensing of Environment*, *20*, 121−139.

Tucker, C. J. (1979). Red and photographic infrared linear combinations for monitoring vegetation. *Remote Sensing of Environment*, *8*, 127−150.

Ünsalan, C., & Boyer, K. L. (2004). Linearized vegetation indices based on a formal statistical framework. *IEEE Transactions on Geoscience and Remote Sensing*, *42*, 1575−1585.

Verhoef, W. (1984). Light scattering by leaf layers with application to canopy reflectance modeling: The SAIL model. *Remote Sensing of Environment*, *16*, 125−141.

Verstraete, M. M., & Pinty, B. (1991). The potential contribution of satellite remote sensing to the understanding of arid lands processes. *Vegetation*, *91*, 59−72.

Verstraete, M. M., Pinty, B., & Myneni, R. B. (1996). Potential and limitation of information extraction on the terrestrial biosphere from satellite remote sensing. *Remote Sensing of Environment*, *58*, 201−214.

Wittich, K. -P., & Hansing, O. (1995). Area-averaged vegetative cover fraction estimated from satellite data. *International Journal of Biometeorology*, *38*, 209−215.

Wood, E. F., & Lakshmi, E. (1993). Scaling water and energy fluxes in climate systems: Three land-atmospheric modeling experiments. *Journal of Climate*, *6*, 839−857.